

Robust synchronization of electric power generators^{*}

Olaoluwapo Ajala^{a,2}, Alejandro D. Domínguez-García^{a,b,2} and Daniel Liberzon^{a,b,*,1}

^aDepartment of Electrical and Computer Engineering, University of Illinois at Urbana-Champaign, Urbana, IL 61801, U.S.A.

^bCoordinated Science Laboratory, University of Illinois at Urbana-Champaign, Urbana, IL 61801, U.S.A.

ARTICLE INFO

Keywords:

Robust synchronization
Input-to-State stability
Synchronous generators.

ABSTRACT

We consider the problem of synchronizing two electric power generators, one of which (the leader) is serving a time-varying electrical load, so that they can ultimately be connected to form a single power system. Each generator is described by a second-order reduced state-space model. We assume that the generator not serving an external load initially (the follower) has access to measurements of the leader's phase angle, corrupted by some additive disturbances. By using these measurements, and leveraging results on reduced-order observers with ISS-type robustness, we propose a procedure that drives (i) the angular velocity of the follower close enough to that of the leader, and (ii) the phase angle of the follower close enough to that of the point at which both systems will be electrically connected. An explicit bound on the synchronization error in terms of the measurement disturbance and the variations in the electrical load served by the leader is computed. We illustrate the procedure via numerical simulations.

1. Introduction

Research into synchronization of dynamical systems originates in the 17th century study of pendulum clocks by Huygens and continues vigorously to this day, driven by theoretical interest and applications in mechanical and electrical systems, multi-agent coordination, teleoperation, haptics, and other fields. In the physics literature, the famous Pecora-Carroll synchronization scheme has generated a lot of activity, some of which was recently surveyed in [21]. In modern control-theoretic literature, tools that have been prominent in addressing synchronization problems are dissipativity theory [6, 4, 8] and observer design [20, 22, 5]. In the context of electric power systems, Kuramoto-type models of coupled phase oscillators, which have been utilized in numerous areas since first proposed in [19], are also starting to be adopted to describe the behavior of inertia-less microgrids (see, e.g., [26, 9, 24, 29, 10, 32] and the references therein).

It is important to distinguish between two basic synchronization scenarios. The first one is when there is bidirectional exchange of information between systems that are already coupled (usually by mechanical or electrical forces) and are trying to achieve a common objective; see, e.g., [9, 30, 23]. The second scenario is when the flow of information is unidirectional: from a "leader" to a "follower." In this case, the follower and the leader are not physically coupled

at first, but the follower is trying to emulate the behavior of the leader so as to attempt physical coupling. This second setting naturally arises in the problem of connecting an electrical generator to an electrical network, and it is the focus of this paper.

One often needs to guarantee an acceptable level of synchronization in the presence of errors affecting the measurements exchanged between the uncoupled systems trying to synchronize. Such *robust synchronization* problems have recently been receiving attention in the literature. Systems in Lurie form satisfying a passifiability assumption on the linear part were treated in [12, 11]. The work reported in [22] establishes robustness of synchronization to uncertainties satisfying inequality constraints and relies on Lyapunov-based observer design. On the other hand, as discussed in [7], most known synchronization schemes are quite sensitive to even small random noise, and not many general results addressing their robustness to bounded disturbances are presently available. The recent work [5] addresses this problem using an ISS observer approach developed earlier in [25], which also serves as a conceptual basis for the synchronization scheme to be presented here. For electric power generators, robust synchronization methods are necessary due to disturbances in the measured voltage, frequency and phase of the connection points, which can potentially result in damage to electrical components and propagation of disturbances across the power system [28].

In this paper, we consider two power systems that are not electrically connected, with the ultimate goal of interconnecting them to form a single system with all its generators being synchronized. Here, we focus on the case when the first system, referred to as the leader, is comprised of one generator and one load, both of which are connected to a bus with voltage support; and the second system, referred to as the follower, is comprised of a single generator with similar voltage support. The objective is to synchronize both systems, i.e., make the generators rotate at the same angular velocity, and make the phase angle of the point at which

^{*} A preliminary version of this paper was presented at the 57th IEEE Conference on Decision and Control (CDC 2018).

^{*}Corresponding author

✉ oaja1a2@ILLINOIS.EDU (O. Ajala); a1edan@ILLINOIS.EDU (A.D.

Domínguez-García); liberzon@ILLINOIS.EDU (D. Liberzon)

ORCID(s): 0000-0001-9557-3247 (A.D. Domínguez-García);

0000-0003-2383-0114 (D. Liberzon)

¹Daniel Liberzon's work was supported by the NSF grant CMMI-1662708 and the AFOSR grant FA9550-17-1-0236.

²The work done by Olaoluwapo Ajala and Alejandro D. Domínguez-García was supported by the Advanced Research Projects Agency-Energy (ARPA-E), U.S. Department of Energy, within the NODES program, under Award DE-AR0000695.

they will be interconnected match. Once these two objectives are achieved, it is possible to electrically connect the follower system to the leader system without causing large currents to flow across both systems, or causing mechanical components to break (see, e.g., [28]).

By assuming the load in the leader system is not varying too rapidly, we first show that a standard integral control stabilizes the angular velocity of the generator in the leader system. Then, by assuming the follower system has access to only phase measurements (but not angular velocity measurements) of the leader system, we show that even if the phase measurements are corrupted, due to, e.g., noise or a malicious cyber attack, the generator in the follower system will be able to bring its angular velocity close enough to that of the generator in the leader system. As for phase synchronization, our procedure cannot guarantee that the phase difference will converge to within some small value around zero; in fact, the opposite is generally true—the phase difference will grow unbounded over time. However, this is not a problem in practice, since one just needs to wait until the phase difference is a multiple of 2π to physically interconnect both systems.

A preliminary study of the basic control design and synchronization methods presented in this work was first conducted in [3]. Nonetheless, the presentation given in this paper is more complete and includes additional analytical and numerical results (see [1, 2] for a derivation of the generator model used in our analysis). The more general case when the generator damping function is phase-dependent is also studied.

The paper is organized as follows. In Section 2, we present the mathematical models used and discuss the assumptions made in the problem formulation. In Section 3, we design and analyze feedback control laws for solving the synchronization problem. In Section 4, implementation aspects are discussed and numerical results are presented to validate our proposed control law and synchronization method. In Section 5, we show that our method is applicable to a more general class of problems, i.e., when the damping coefficients in the models are phase-dependent rather than constant. Section 6 concludes the paper.

2. System description

We focus on the task of synchronizing two electric power generators, with the first one serving an electrical load via a node referred to as the “bus,” and the second one trying to connect to the bus. The synchronization task is depicted in Fig. 1.

Let ω_1 denote the angular speed of the first generator (in electrical radians per second), let θ_1 denote the absolute phase angle of generator 1, and let δ_1 denote its relative phase angle, both in radians. This means that

$$\delta_1 := \theta_1 - \omega_0 t, \quad (1)$$

where ω_0 denotes some nominal frequency; thus, we have

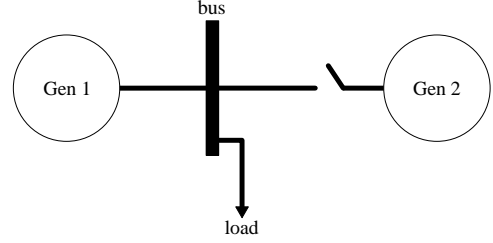


Figure 1: Synchronization of two generators: a leader and a follower.

$\dot{\theta}_1 = \omega_1$, so that

$$\dot{\delta}_1 = \omega_1 - \omega_0. \quad (2)$$

The corresponding variables ω_2 , θ_2 , δ_2 for the second generator are defined in the same way. We denote by θ_3 the absolute phase angle of the bus voltage. We also define the relative phase angle of the bus voltage as

$$\delta_3 := \theta_3 - \omega_0 t, \quad (3)$$

and we have $\dot{\theta}_3 = \omega_3$, so that $\dot{\delta}_3 = \omega_3 - \omega_0$, where ω_3 is the frequency of the bus (in electrical radians per second).

We consider the following second-order reduced model for the first generator (see [2] for model derivation details):

$$\dot{\theta}_1 = \omega_1, \quad (4)$$

$$\dot{\omega}_1 = u_1 - \ell(t) - D_1^{(0)} \omega_1, \quad (5)$$

where u_1 is the control input;

$$\ell(t) = B_1(\theta_{13}(t)) + D_1(\theta_{13}(t)) \cdot \dot{\theta}_{13}(t) \quad (6)$$

is the electrical load;

$$\theta_{13}(t) := \theta_1(t) - \theta_3(t) \quad (7)$$

is the difference between the absolute phase angles of the first generator and the bus; B_1 is a globally bounded and globally Lipschitz function given by

$$B_1(s) := K_1 \sin(s) + X_1 \sin(2s), \quad (8)$$

where K_1 is a positive constant and X_1 is a nonnegative constant [2]; the damping function D_1 is a globally bounded and globally Lipschitz function given by

$$D_1(s) = C_1 \cos^2(s) + C_2 \sin^2(s), \quad (9)$$

where C_1 and C_2 are positive constants [2]; and $D_1^{(0)}$ is a positive constant.³

From the generator dynamic model in (4) and (5), the definition (7), and the resulting relation

$$\dot{\theta}_{13}(t) := \dot{\theta}_1(t) - \dot{\theta}_3(t) = \omega_1 - \omega_3, \quad (10)$$

³ $D_1^{(0)} := \bar{D}_1^{(0)} + \bar{D}_1^{(0)}$, where $\bar{D}_1^{(0)}$ represents the friction and windage damping coefficient of the generator, and $\bar{D}_1^{(0)} := \frac{1}{R_D \omega_0}$, where R_D represents the droop coefficient of the generator (see [2] for more details).

it is easy to see that the dynamical model for the bus takes the form

$$\dot{\theta}_3 = \omega_3, \quad (11)$$

$$\dot{\omega}_3 = u_1 - \ell(t) - D_1^{(0)}\omega_1 - \ddot{\theta}_{13}(t). \quad (12)$$

The second-order reduced model for the second generator (before it is connected) is analogous to (4), (5) but with no electrical load term, i.e.,

$$\dot{\theta}_2 = \omega_2, \quad (13)$$

$$\dot{\omega}_2 = u_2 - D_2^{(0)}\omega_2, \quad (14)$$

where u_2 is the control input and $D_2^{(0)}$ is a positive constant.

The synchronization task consists in ensuring that the phase and angular speed of the second generator match those of the bus. Accordingly, from now on we refer to the bus modeled by (11), (12) as the *leader*, and the second generator modeled by (13), (14) as the *follower*. We make the following assumption on the initial condition of the leader-follower system depicted in Fig. 1.

Assumption 1 At the initial time t_0 (the time when our control strategy will be initialized), generator 1 operates in steady state corresponding to some constant load $\bar{\ell}$ that is within the range of the function $B_1(\cdot)$.

In view of the power balance equation (6), Assumption 1 means that $\theta_{13}(t_0)$ equals the solution $\bar{\theta}_{13}$ of the equation $\bar{\ell} = B_1(\bar{\theta}_{13})$, and that $\dot{\theta}_{13}(t_0) = \omega_1(t_0) - \omega_3(t_0) = 0$. [Indeed, $\theta_{13}(t) \equiv \bar{\theta}_{13}$ is the unique solution of the ODE $\dot{\ell} = B_1(\theta_{13}(t)) + D_1(\theta_{13}(t)) \cdot \theta_{13}(t)$ starting at $\bar{\theta}_{13}$.] For $t \geq t_0$, we allow the load $\ell(t)$ to change according to the following assumption.

Assumption 2 For some positive constants Δ_ℓ and $\Delta_{\dot{\ell}}$, we have:

$$|\ell(t) - \bar{\ell}| \leq \Delta_\ell, \quad |\dot{\ell}(t)| \leq \Delta_{\dot{\ell}}. \quad (15)$$

Letting $\Delta\theta \approx \theta_{13}(t) - \bar{\theta}_{13}$, $\Delta\dot{\theta} \approx \omega_1(t) - \omega_3(t)$, $\Delta\ell \approx \ell(t) - \bar{\ell}$, and $\Delta\dot{\ell} \approx \dot{\ell}(t)$ denote small perturbations about the initial values, one can show, by small-signal analysis, that

$$\begin{aligned} \frac{d}{dt} \begin{pmatrix} \Delta\theta \\ \Delta\dot{\theta} \end{pmatrix} &= \begin{pmatrix} -\frac{B_1'(\bar{\theta}_{13})}{D_1(\bar{\theta}_{13})} \\ \left(\frac{B_1'(\bar{\theta}_{13})}{D_1(\bar{\theta}_{13})}\right)^2 \end{pmatrix} \Delta\theta \\ &+ \begin{pmatrix} \frac{1}{D_1(\bar{\theta}_{13})} & 0 \\ -\frac{B_1'(\bar{\theta}_{13})}{(D_1(\bar{\theta}_{13}))^2} & \frac{1}{D_1(\bar{\theta}_{13})} \end{pmatrix} \begin{pmatrix} \Delta\ell \\ \Delta\dot{\ell} \end{pmatrix}, \end{aligned} \quad (16)$$

and if Δ_ℓ and $\Delta_{\dot{\ell}}$ in (15) are sufficiently small then, at least on some finite time horizon, there exist positive constants Δ_θ and $\Delta_{\dot{\theta}}$ such that

$$|\theta_{13}(t) - \bar{\theta}_{13}| \leq \Delta_\theta, \quad |\dot{\theta}_{13}(t)| = |\omega_1(t) - \omega_3(t)| \leq \Delta_{\dot{\theta}}. \quad (17)$$

We henceforth utilize the existence of Δ_θ and $\Delta_{\dot{\theta}}$. Refer to Section 4.4 for more information on this.

Signal measurements

We make the following assumption on the signal measurements received by the follower system.

Assumption 3 A phasor-measurement unit (PMU) is used to measure the absolute angle of the “bus” node, which is corrupted by a measurement disturbance, $d(t)$. Also, the steady-state value $\bar{\theta}_{13}$ is known to the follower (through the knowledge of $\bar{\ell}$), but angular speed measurements are not available to the follower.

One major potential source of the disturbance alluded to in Assumption 3 is *spoofing* [17], but it can also be due to a combination of several sources. Thus, phase measurements available to the follower take the form

$$\theta_3(t) + d(t), \quad (18)$$

where $d(t)$ is an unknown disturbance, with $\theta_3(t) + d(t) \in [0, 2\pi)$.⁴ Our goal is to achieve robust synchronization in the face of the unknown disturbance $d(t)$, and to quantitatively characterize how the synchronization error is affected by the size of this disturbance.

3. Controlled synchronization

In this section, a feedback control law is designed for the leader, and a synchronization method is developed for the follower system.

3.1. Control design and analysis

First generator and bus (leader)

Note that the first generator and the bus share the same control input. The purpose of this control is to drive the bus frequency $\omega_3(t)$ to the nominal frequency value ω_0 . In view of the second bound in (17), if Δ_θ is small then this goal can also be approximately achieved by driving the angular speed $\omega_1(t)$ of the first generator to ω_0 . This suggests the following control input:

$$u_1(t) = -k\delta_1(t) = -k(\theta_1(t) - \omega_0 t), \quad k > 0. \quad (19)$$

Since the dynamics of $\delta_1(t)$ are given by (2), it is easy to recognize in (19) a standard integral control law for making $\omega_1(t)$ asymptotically track the constant reference ω_0 . Under the action of this control, the first generator reduced-order model (4), (5) becomes:

$$\dot{\theta}_1 = \omega_1, \quad (20)$$

$$\dot{\omega}_1 = -k\theta_1 + k\omega_0 t - \ell(t) - D_1^{(0)}\omega_1. \quad (21)$$

To validate the control law (19), we want to show that the solutions of the closed-loop system given by (2), (20)

⁴Note that if the unknown disturbance is caused by a spoofing attack on the GPS signal of the PMU, it might be possible to refine the upper bound on $d(t)$. For example, in [17], it was shown that a spoofing attack can be engineered so as to perturb the phase measurement provided by the PMU by as much as 0.25π rad without being detected; thus, in such a case, one could assume $d(t) \in (-0.25\pi, 0.25\pi)$.

and (21) are bounded and that $\omega_1(t)$ is regulated to ω_0 in an appropriate sense. To this end, it is convenient to rewrite the (ω_1, δ_1) -dynamics as follows:

$$\begin{pmatrix} \dot{\omega}_1 \\ \dot{\delta}_1 \end{pmatrix} = \begin{pmatrix} -D_1^{(0)} & -k \\ 1 & 0 \end{pmatrix} \begin{pmatrix} \omega_1 \\ \delta_1 \end{pmatrix} - \begin{pmatrix} \ell(t) \\ \omega_0 \end{pmatrix},$$

which we can view as a linear time-invariant system driven by a time-varying perturbation that creates a time-varying equilibrium at

$$\omega_1 = \omega_0, \quad \delta_1 = -\frac{\ell(t) + D_1^{(0)}\omega_0}{k} =: \delta_0(t) \quad (22)$$

(meaning that for each frozen time t , this is the equilibrium of the corresponding fixed affine system). Let us shift the center of coordinates to this time-varying equilibrium by defining

$$\bar{\omega}_1(t) := \omega_1(t) - \omega_0, \quad \bar{\delta}_1(t) := \delta_1(t) - \delta_0(t). \quad (23)$$

Note that small values of $\bar{\omega}_1(t)$ correspond to $\omega_1(t)$ being regulated close to the nominal frequency ω_0 . The following result formally describes in what sense our controller achieves this goal.

Proposition 1 *For each $k > 0$ there exist constants $c, \lambda > 0$ such that the closed-loop system variables, $\bar{\omega}_1$ and $\bar{\delta}_1$, satisfy the steady-state bound*

$$\limsup_{t \rightarrow \infty} \left\| \begin{pmatrix} \bar{\omega}_1(t) \\ \bar{\delta}_1(t) \end{pmatrix} \right\| \leq \frac{c\Delta_{\ell}}{\lambda k}, \quad (24)$$

where Δ_{ℓ} comes from (15).

Proof (sketch, see [3, 1] for details): In the new coordinates $(\bar{\omega}_1, \bar{\delta}_1)$, the closed-loop dynamics become

$$\begin{pmatrix} \dot{\bar{\omega}}_1 \\ \dot{\bar{\delta}}_1 \end{pmatrix} = A \begin{pmatrix} \bar{\omega}_1 \\ \bar{\delta}_1 \end{pmatrix} + \begin{pmatrix} 0 \\ \nu(t) \end{pmatrix}, \quad (25)$$

where

$$A := \begin{pmatrix} -D_1^{(0)} & -k \\ 1 & 0 \end{pmatrix}, \quad \nu(t) := \frac{\dot{\ell}(t)}{k}. \quad (26)$$

Since A is Hurwitz, there exist constants $c, \lambda > 0$ (which depend on k) such that for all t we have⁵

$$\|e^{At}\| \leq ce^{-\lambda t}. \quad (27)$$

Computation of c and λ is addressed in Section 4.1. Our system (25) is the LTI system $\dot{x} = Ax$ driven by the perturbation ν which, in view of the second bound in (15), satisfies $|\nu(t)| \leq \Delta_{\ell}/k$ for all $t \geq 0$. It is well known and straightforward to derive that c/λ is an upper bound on the system's \mathcal{L}_{∞} -induced gain, and in particular, $c\Delta_{\ell}/(\lambda k)$ is the ultimate bound on the norm of the solution in steady state as claimed in (24). \square

⁵Here $\|\cdot\|$ stands for the induced matrix norm corresponding to the Euclidean norm.

Second generator (follower)

For the follower (second generator) described by (13), (14), we would like to define the control input $u_2(t)$ so as to make the angular speed $\omega_2(t)$ synchronize with the bus frequency $\omega_3(t)$. Since in view of the second bound in (17) the frequencies $\omega_3(t)$ and $\omega_1(t)$ are close to each other, it is reasonable to base the design of u_2 on the (somewhat simpler) dynamics of the first generator instead of those of the bus. Let us use (6) to rewrite the equation (21) as

$$\begin{aligned} \dot{\omega}_1 &= -k\theta_1 + k\omega_0 t - B_1(\theta_{13}(t)) \\ &\quad - D_1(\theta_{13}(t)) \cdot \dot{\theta}_{13} - D_1^{(0)}\omega_1. \end{aligned} \quad (28)$$

We can make the dynamics (14) of ω_2 approximately match these dynamics of ω_1 by doing the following: (i) approximating $\theta_1(t)$ (which is not available to the follower) by $\theta_3(t) + d(t) + \bar{\theta}_{13}$ —this makes sense since $\theta_3(t) + d(t)$ are the approximate measurements of $\theta_3(t)$ available to the follower, and $\bar{\theta}_{13}$ approximates the difference $\theta_{13}(t) = \theta_1(t) - \theta_3(t)$ in the sense of the first bound in (17) and is also available to the follower; (ii) approximating $B_1(\theta_{13}(t))$ by $B_1(\bar{\theta}_{13})$; (iii) correcting the difference between the damping constants $D_1^{(0)}$ and $D_2^{(0)}$; and (iv) ignoring the term $D_1(\theta_{13}(t)) \cdot \dot{\theta}_{13}$ which is bounded by virtue of (9) and (17). This suggests the following control input:

$$\begin{aligned} u_2(t) &= -k\left(\theta_3(t) + d(t) + \bar{\theta}_{13}\right) + k\omega_0 t \\ &\quad - B_1(\bar{\theta}_{13}) + \left(D_2^{(0)} - D_1^{(0)}\right)\omega_2(t). \end{aligned}$$

We can then write the closed-loop dynamics of the follower as

$$\begin{aligned} \dot{\theta}_2 &= \omega_2, \\ \dot{\omega}_2 &= -k\left(\theta_3(t) + d(t) + \bar{\theta}_{13}\right) + k\omega_0 t - B_1(\bar{\theta}_{13}) \\ &\quad - D_1^{(0)}\omega_2. \end{aligned} \quad (29)$$

This choice of control for the follower will be validated by the synchronization analysis given next.

Remark 1 The above control design for the follower is not dependent on the particular form of the control u_1 for the leader, but only on the fact that this control depends just on the angle θ_1 and not on the angular velocity ω_1 , so that the follower can approximately reconstruct this control (modulo the disturbance). We also see that the exact nature of the damping term in the follower model is not important because it is canceled by control.

3.2. Synchronization analysis

Since we are interested in synchronizing the angular velocity ω_2 of the follower to the frequency ω_3 of the leader, we consider the synchronization error

$$e(t) := \omega_2(t) - \omega_3(t). \quad (31)$$

The following result characterizes the quality of synchronization in terms of the size of the disturbance $d(t)$, the control gain k , the damping coefficient $D_1^{(0)}$, and the various constants appearing in (8), (9), and (17).

Proposition 2 *Along the closed-loop dynamics of the leader and the follower defined in Section 3.1, the synchronization error (31) satisfies the steady-state bound*

$$\limsup_{t \rightarrow \infty} |e(t)| \leq \frac{1}{D_1^{(0)}} \left(k \limsup_{t \rightarrow \infty} |d(t)| + (C_1 + C_2 + D_1^{(0)})\Delta_{\dot{\theta}} + (k + K_1 + 2X_1)\Delta_{\theta} \right). \quad (32)$$

This bound shows, in particular, that the gain from the measurement disturbance d to the synchronization error e is proportional to the control gain k , thus decreasing k reduces the effect of this disturbance on synchronization (especially when the damping coefficient $D_1^{(0)}$ is small). On the other hand, decreasing k has a negative effect on closed-loop stability of the first generator, as can be seen from the eigenvalues of the matrix A defined in (26) and from the bound (24). This gives the interesting insight that, to mitigate the effect of this disturbance, we may want to (temporarily) reduce the control gain k during the synchronization stage.

Proof: We find it convenient to split e as

$$e = (\omega_2 - \omega_1) + (\omega_1 - \omega_3) =: e_{21} + e_{13} \quad (33)$$

and analyze the two components separately. For e_{13} , we already have the second bound from (17) which says that

$$|e_{13}(t)| \leq \Delta_{\dot{\theta}}. \quad (34)$$

For e_{21} , using (30), (28), and (7) we have (suppressing all time arguments for simplicity)

$$\begin{aligned} \dot{e}_{21} &= \dot{\omega}_2 - \dot{\omega}_1 \\ &= B_1(\theta_{13}) - B_1(\bar{\theta}_{13}) + D_1(\theta_{13}) \cdot \dot{\theta}_{13} \\ &\quad - D_1^{(0)} e_{21} + k(\theta_{13} - \bar{\theta}_{13}) - kd. \end{aligned} \quad (35)$$

Let us define the candidate Lyapunov function

$$V(e_{21}) := \frac{1}{2} e_{21}^2.$$

Its derivative along solutions of (35) satisfies the inequality

$$\begin{aligned} \dot{V} &\leq -D_1^{(0)} e_{21}^2 + \left(k|\theta_{13} - \bar{\theta}_{13}| + k|d| + |B_1(\theta_{13}) \right. \\ &\quad \left. - B_1(\bar{\theta}_{13})| + |D_1(\theta_{13})| \cdot |\dot{\theta}_{13}| \right) |e_{21}|. \end{aligned} \quad (36)$$

Recall that $D_1^{(0)} > 0$. By the first bound in (17) we have $|\theta_{13} - \bar{\theta}_{13}| \leq \Delta_{\theta}$. Furthermore, since B_1 defined in (8) is globally Lipschitz with Lipschitz constant $K_1 + 2X_1$, we also have $|B_1(\theta_{13}) - B_1(\bar{\theta}_{13})| \leq (K_1 + 2X_1)\Delta_{\theta}$. Finally, D_1 defined in (9) is globally bounded by $C_1 + C_2$ which, combined with the second bound in (17), gives $|D_1(\theta_{13})| \cdot |\dot{\theta}_{13}| \leq (C_1 + C_2)\Delta_{\dot{\theta}}$. Plugging all these bounds into (36), we obtain

$$\dot{V} \leq -D_1^{(0)} e_{21}^2 + \left(k|d| + (k + K_1 + 2X_1)\Delta_{\theta} \right.$$

$$\begin{aligned} &\left. + (C_1 + C_2)\Delta_{\dot{\theta}} \right) |e_{21}| \\ &= -D_1^{(0)} |e_{21}| \left(|e_{21}| - \frac{k|d| + (k + K_1 + 2X_1)\Delta_{\theta} + (C_1 + C_2)\Delta_{\dot{\theta}}}{D_1^{(0)}} \right), \end{aligned}$$

which implies that, for an arbitrary choice of $\varepsilon \geq 0$, we have

$$\begin{aligned} |e_{21}| &> \frac{k|d|}{D_1^{(0)}} (1 + \varepsilon) \\ &+ \frac{(C_1 + C_2)\Delta_{\dot{\theta}} + (k + K_1 + 2X_1)\Delta_{\theta}}{D_1^{(0)}} (1 + \varepsilon) \end{aligned} \quad (37)$$

$$\Rightarrow \dot{V} < -D_1^{(0)} \frac{2\varepsilon}{1 + \varepsilon} V. \quad (38)$$

The standard ISS analysis (see, e.g., [27]) now implies that $e_{21}(t)$ stays bounded and satisfies the ultimate bound

$$\begin{aligned} \limsup_{t \rightarrow \infty} |e_{21}(t)| &\leq \frac{1}{D_1^{(0)}} \left(k \limsup_{t \rightarrow \infty} |d(t)| \right. \\ &\quad \left. + (C_1 + C_2)\Delta_{\dot{\theta}} + (k + K_1 + 2X_1)\Delta_{\theta} \right). \end{aligned}$$

Combining this with (33) and (34), we arrive at the desired bound (32). \square

Remark 2 The calculations given in the proof of Proposition 2 can also be used to upper-bound the time that one must wait before satisfactory angular velocity matching is achieved. Indeed, as long as the inequality (37) is satisfied, the bound (38) implies that $e_{21}(t)$ decreases exponentially according to

$$|e_{21}(t)| \leq e^{-D_1^{(0)} \frac{\varepsilon}{1 + \varepsilon} (t - t_0)} \omega_0$$

where we used $e_{21} = \omega_2 - \omega_1$ and the fact that, at time t_0 , the first generator is assumed to be operating in steady state (see Assumption 1) so that its angular velocity ω_1 is close to the nominal value ω_0 , while the second generator is at rest so that $\omega_2(t_0) = 0$. Combined with (33) and (34), this gives us a (possibly quite conservative) estimate on the time before the mismatch between the angular velocities of the leader and the follower becomes close to its steady-state value.

4. Implementation and numerical results

In this section, parameters for the proposed control law and synchronization method are evaluated, the synchronization procedure is discussed, the post-synchronization system is described, and numerical results are provided. The numerical results are developed as follows: with initial conditions of the leader system set to an equilibrium state and that of the follower system set to zero, the simulation starts at time $t = 0$ s with the electrical load at a nominal value of 0.5 pu,

where “pu” denotes per-unit.⁶ At time $t = 5$ s, the load is perturbed about the nominal value, with the change in size and speed constrained to $|\ell(t) - 0.5| \leq \Delta_\ell$ and $|\dot{\ell}(t)| = \Delta_{\dot{\ell}}$, respectively, where Δ_ℓ and $\Delta_{\dot{\ell}}$ are positive constants. Using a base power of 2.2 MW for the system, a base voltage amplitude of 480 V for the generators, and a base voltage amplitude of 230 kV for the bus, the model parameters are: $k = 0.01$, $\omega_0 = 120\pi$ rad/s, $D_1^{(0)} = D_2^{(0)} = 0.0531$ s/rad, $\bar{\ell} = 0.5$ pu, $K_1 = 0.6434$ pu, $K_2 = 0.4167$ pu, $X_1 = 0.0742$ pu, $X_2 = 0.0742$ pu, $C_1 = 0.0656$ pu, $C_2 = 0.00548$ pu, and $\bar{\theta}_{13} = 0.7245$ rad.

4.1. Parameter evaluation

The values of λ and c in (27) can be easily estimated as follows (see [3, 1] for details). We impose the following assumption on the control gain k .

Assumption 4 The control gain is chosen to satisfy $k \geq (D_1^{(0)})^2/4$ so that the eigenvalues of the matrix A , from (26), are complex with real parts $-\frac{1}{2}D_1^{(0)}$.

Following from Assumption 4, we can take the stability margin (i.e., exponential decay rate) λ appearing in (27) to be

$$\lambda := \frac{1}{2}D_1^{(0)}.$$

(Note that for values of k closer to 0 the stability margin would decrease.) For the overshoot constant c in (27), we can obtain the following estimate:

$$c = \sqrt{\frac{k + 1 + \sqrt{(k - 1)^2 + (D_1^{(0)})^2}}{k + 1 - \sqrt{(k - 1)^2 + (D_1^{(0)})^2}}}.$$

Utilizing these formulas and the chosen model parameters, we have that $c = 10.3796$ and $\lambda = 0.0266$.

4.2. Synchronization procedure

In addition to angular velocity synchronization, phase synchronization is also important. The phase θ_2 will evolve according to (29), which comes from the physics of the system but was not explicitly taken into account in the above procedure. Due to the imperfect frequency synchronization caused by the disturbance, the phase difference $\theta_2 - \theta_3$ will “drift” and there will be a time when $\theta_2(t) - (\theta_3(t) + d(t))$ will become close to an integer multiple of 2π . The idea is that we will detect when this happens at the follower’s side by looking at the measurements $\theta_3 + d$ and comparing them with θ_2 , and at that moment we will connect the second generator.

⁶System quantities expressed in per-unit have been normalized as fractions of a defined base quantity, and the rated value of the system quantity is usually chosen as the base quantity. In other words, for a system whose rated power capacity and voltage are 10 W and 480 V, respectively, a power measurement of 0.5 pu is equivalent to 5 W, and a voltage measurement of 1 pu is equivalent to 480 V [18].

For some disturbances that oscillate around 0, it is possible in principle that $\theta_2(t) - (\theta_3(t) + d(t))$ will remain bounded and will never become a multiple of 2π . However, for most disturbances—including constant-sign offsets arising from spoofing [17]—the procedure is guaranteed to work. Indeed, assuming the load is nearly constant, the most relevant component e_{21} of the synchronization error will satisfy (approximately) the simplified equation $\dot{e}_{21} = -D_1^{(0)}e_{21} - kd(t)$. Now, if $d(t)$ is either a constant nonzero offset, or oscillates around a constant nonzero offset, then $e_{21}(t)$ will also have a nonzero average. Integrating it, we see that $\theta_2(t) - \theta_1(t)$ will grow unbounded, as needed.

4.3. Post-synchronization system

As the leader and follower are synchronized and connected to form a single power system, the models governing the behavior of the two generators change. The dynamics of the first generator are now described by

$$\begin{aligned} \dot{\theta}_1 &= \omega_1, \\ \dot{\omega}_1 &= u_1 - B_1(\theta_{13}(t)) - D_1(\theta_{13}(t)) \cdot \dot{\theta}_{13}(t) - D_1^{(0)}\omega_1, \end{aligned} \quad (39)$$

the dynamics of the second generator are described by

$$\begin{aligned} \dot{\theta}_2 &= \omega_2, \\ \dot{\omega}_2 &= u_2 - B_2(\theta_{23}(t)) - D_2(\theta_{23}(t)) \cdot \dot{\theta}_{23}(t) - D_2^{(0)}\omega_2, \end{aligned} \quad (40)$$

and the power balance equation for the system is

$$\begin{aligned} \ell(t) &= B_1(\theta_{13}(t)) + D_1(\theta_{13}(t)) \cdot \dot{\theta}_{13}(t) \\ &\quad + B_2(\theta_{23}(t)) + D_2(\theta_{23}(t)) \cdot \dot{\theta}_{23}(t), \end{aligned} \quad (41)$$

where B_2 and D_2 are globally bounded and globally Lipschitz functions, taking the same form as B_1 and D_1 , and

$$\theta_{23}(t) := \theta_2(t) - \theta_3(t) \quad (42)$$

is the difference between the absolute phase angles of the second generator and the bus.

After the leader and follower are successfully synchronized, interconnected, and the system states approach a stable equilibrium, the control input of the leader and follower is typically modified to ensure that the power consumed by the electrical load is shared, by the generators, according to participation factors (see [31], pp. 345–356, for more details).

4.4. Numerical results

Firstly, we present numerical results that show the effects of load change on control performance. In relation to (15) and (17), the numerical results depicted in Figs. 2a and 2b suggest that there is a strong coupling between Δ_θ and variables Δ_ℓ and $\Delta_{\dot{\ell}}$, and between Δ_θ and Δ_ℓ . However, there is a weak coupling between Δ_θ and $\Delta_{\dot{\ell}}$. In Fig. 2c, the deviation of the bus frequency from nominal value is investigated and compared to the bound required by the IEEE 1547 standard, i.e. $|\omega_3(t) - \omega_0| \leq \pi$, and the effects of Δ_ℓ and $\Delta_{\dot{\ell}}$ on the frequency of the bus are recorded. The results show

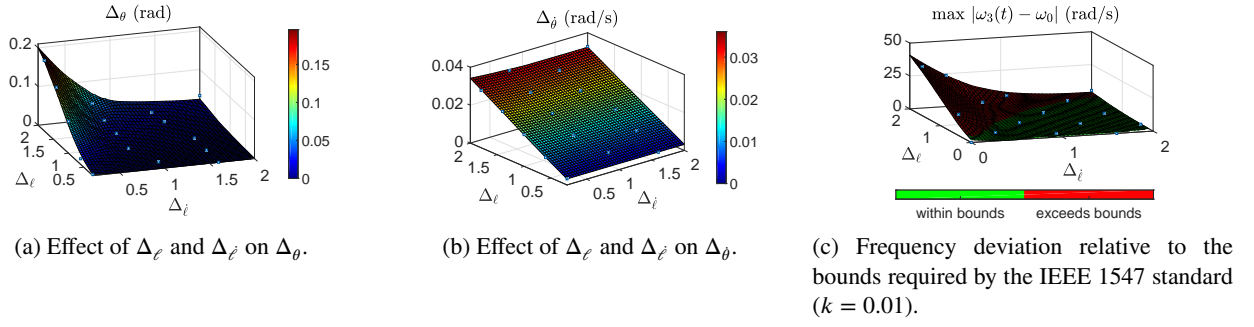


Figure 2: Effects of load change on control performance

Table 1
Theoretical Steady State Bounds for Synchronization Error

| $d(t)$ | Theoretical Bounds for $e(t)$ |
|----------------|-------------------------------|
| 0.125π rad | 0.131π rad/s |
| 0.25π rad | 0.1546π rad/s |
| 0.5π rad | 0.2017π rad/s |

that, for each fixed value of $\Delta_{\dot{\theta}}$, the controller performance improves when Δ_ℓ decreases, and for each fixed value of Δ_ℓ , the controller performance improves when $\Delta_{\dot{\theta}}$ increases. Although Fig. 2c suggests a weaker coupling between $\Delta_{\dot{\theta}}$ and the controller performance, this result appears to contradict the bound in (24). However, it is important to note that this bound also takes into account the effects of phase deviations from a nominal value.

In Fig. 3, the observed synchronization error before the leader and follower are interconnected is shown, and in Fig. 4, the bus frequency of the electrical power system is depicted. These numerical results are for three constant disturbance values, $d(t) = 0.125\pi$ rad, $d(t) = 0.25\pi$ rad, and $d(t) = 0.5\pi$ rad.⁷ In these results, the second generator has an initial frequency of 0 rad/s, whereas the initial value of the bus frequency is ω_0 , the nominal value. As a result, the synchronization error is $-\omega_0$ at $t = 0$ s.

In Figs. 3 and 4, the leader and follower are interconnected only when (i) the observed phase difference of the connection points, $|\theta_2(t) - \theta_3(t) - d(t)|$, is a multiple of 2π and (ii) the synchronization error is within the admissible limits specified in [14], i.e. $|e(t)| \leq 0.134\pi$ rad/s. After the leader and follower are synchronized and interconnected, the post-synchronization system described in 4.3 is initiated at around $t = 400$ s. The values $\Delta_\ell = 0.01$, $\Delta_{\dot{\theta}} = 0.01$, and $k = 0.01$ are used. Utilizing the main result of Proposition 2, the steady state bounds for the synchronization error are given in Table 1. Comparing these bounds to the admissible limits, i.e. $|e(t)| \leq 0.134\pi$ rad/s, we expect that the leader and follower will synchronize when $d(t) = 0.125\pi$ rad.

⁷We also considered non-constant disturbances oscillating within the same magnitude limits, and observed even better results, suggesting that constant disturbances present a worst-case scenario.

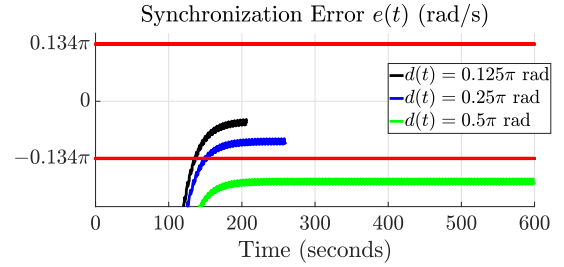


Figure 3: Synchronization error relative to bounds provided in [28, 14].

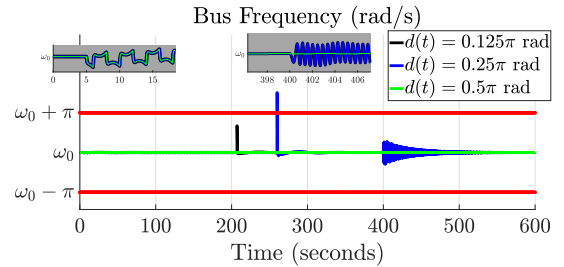


Figure 4: Bus frequency relative to bounds provided in [15].

Examining the results depicted in Fig. 3, we observed that for: (i) $d(t) = 0.125\pi$ rad, the leader and follower successfully synchronized around $t = 200$ s, (ii) $d(t) = 0.25\pi$ rad, the leader and follower successfully synchronized around $t = 260$ s, and (iii) $d(t) = 0.5\pi$ rad, the leader and follower fail to synchronize. This is consistent with the synchronization error bounds listed in Table 1 in the sense that it predicts that the leader and follower will synchronize when $d(t) = 0.125\pi$ rad. The results depicted in Fig. 3 suggest that the proposed synchronization method is robust to large disturbances in phase measurements, even if the disturbance is as large as the maximum resulting from spoofing attacks.

5. Phase-dependent damping

In this section we briefly consider the case when the leader model takes the form

$$\dot{\theta}_1 = \omega_1, \quad (43)$$

$$\dot{\omega}_1 = u_1 - D_1(\theta_1)\omega_1 + \xi_1(t) \quad (44)$$

where u_1 is the control input as before. In contrast with the model (4), (5) considered earlier in the paper, here the damping $D_1(\cdot)$ is phase-dependent, which can arise, e.g., from modeling phase-dependent friction due to eccentricity of the generator rotor. The following assumptions are imposed on the functions $D_1(\cdot)$ and $\xi_1(\cdot)$.

Assumption 5 The function $D_1(\cdot)$ is taken to be periodic with period 2π and it satisfies:

1. There exist numbers $\bar{D}_1 > \underline{D}_1 > 0$ such that $\underline{D}_1 \leq D_1(r) \leq \bar{D}_1$ for all $r \geq 0$.
2. There exists an $\varepsilon > 0$, sufficiently small, such that $|D_1'(r)| \leq \varepsilon$ for all $r \geq 0$.

Assumption 6 $\xi_1(t)$ is a signal whose value is known, and $\dot{\xi}_1(t)$ is uniformly bounded, i.e., there exists an $M > 0$ such that $|\dot{\xi}_1(t)| \leq M$ for all $t \geq 0$.

We note that for the earlier model (4), (5), $\xi_1(t)$ corresponds to the load $\ell(t)$, and having exact knowledge of the load makes the synchronization problem trivial. This is not the case, however, for the case of phase-dependent damping treated here, as we will see shortly.

Next, we take the follower model to be of the form

$$\begin{aligned}\dot{\theta}_2 &= \omega_2, \\ \dot{\omega}_2 &= u_2 - D_2(\theta_2)\omega_2.\end{aligned}$$

The exact form of the function $D_2(\cdot)$ is not important because it will be canceled by the control u_2 . We impose the following assumption on the measurements available to the follower.

Assumption 7 Measurements of the first state θ_1 of the leader are corrupted by an additive disturbance $d(t)$ when being passed to the follower, while measurements of the second state ω_1 are not available to the follower.

5.1. Control design and analysis

We define the control u_1 exactly as before by the equation (19), where the dynamics of $\delta_1(t)$ are given by (2). The closed-loop system (again, (ω_1, δ_1) -dynamics only) is now

$$\begin{pmatrix} \dot{\omega}_1 \\ \dot{\delta}_1 \end{pmatrix} = \begin{pmatrix} -D_1(\theta_1(t)) & -k \\ 1 & 0 \end{pmatrix} \begin{pmatrix} \omega_1 \\ \delta_1 \end{pmatrix} + \begin{pmatrix} \xi_1(t) \\ -\omega_0 \end{pmatrix}$$

which we can view as a linear time-varying system driven by a time-varying perturbation that creates a time-varying equilibrium at

$$\omega_1 = \omega_0, \quad \delta_1 = \frac{\xi_1(t) - D_1(\theta_1(t))\omega_0}{k} =: \delta_0(t) \quad (45)$$

(meaning that for each frozen time t , this is the equilibrium of the corresponding fixed affine system). Shifting the center of coordinates to this time-varying equilibrium by defining the variables $\bar{\omega}_1$ and $\bar{\delta}_1$ as in (23), we obtain the dynamics

$$\begin{pmatrix} \dot{\bar{\omega}}_1 \\ \dot{\bar{\delta}}_1 \end{pmatrix} = A(t) \begin{pmatrix} \bar{\omega}_1 \\ \bar{\delta}_1 \end{pmatrix} + \begin{pmatrix} 0 \\ v(t) \end{pmatrix} \quad (46)$$

where

$$A(t) := \begin{pmatrix} -D_1(\theta_1(t)) & -k \\ 1 & 0 \end{pmatrix} \quad (47)$$

and

$$v(t) := \frac{D_1'(\theta_1(t))\omega_1(t)\omega_0 - \dot{\xi}_1(t)}{k}. \quad (48)$$

We now make the following observations:

1. The matrix $A(t)$ is Hurwitz for each frozen t .
2. Its time derivative

$$\dot{A}(t) = \begin{pmatrix} -D_1'(\theta_1(t))\omega_1(t) & 0 \\ 0 & 0 \end{pmatrix} \quad (49)$$

is small because D_1' was assumed to be small, as long as ω_1 is kept bounded under the action of the control u_1 .

3. The perturbation signal $v(t)$ is bounded for the same reason and also because $\dot{\xi}_1(t)$ is assumed to be bounded (see Assumption 6).

Applying results on stability of slowly time-varying linear systems (see, e.g., [13] and the references therein), we now show that solutions of the closed-loop system are bounded and converge to a small neighborhood of the time-varying equilibrium (45); the size of this neighborhood is determined by the size of the perturbation $v(t)$. This relies on the following well-known result on stability of linear time-varying systems (see, e.g., [16, Theorem 3.4.11]; see also [13] for some extensions).

Lemma 1 Consider the LTV system

$$\dot{x} = A(t)x \quad (50)$$

and assume that:

- $A(t)$ is Hurwitz for each fixed t , and there exist constants $c, \lambda > 0$ such that for all t and s we have $\|e^{A(t)s}\| \leq ce^{-\lambda s}$.
- $A(\cdot)$ is C^1 and uniformly bounded: there exists an $L > 0$ such that $\|A(t)\| \leq L$ for all t .
- $\|\dot{A}(t)\| \leq \mu$ for all t , where $\mu > 0$ is sufficiently small.

Then the system (50) is exponentially stable.

From the proof of the above result given in [16], an upper bound on μ that guarantees stability is obtained as

$$\mu < \beta_1 / (2\beta_2^3) \quad (51)$$

where $\beta_1 := 1/(2L)$, $\beta_2 := c^2/(2\lambda)$. We now develop numerical expressions for these quantities (some calculation details are skipped and can be found in [1]).

In our setting, the matrices $A(t)$ are given by (47) and $D_1(\cdot)$ is assumed to satisfy the lower and upper bounds \underline{D}_1 , \overline{D}_1 . Proceeding analogously to Section 4.1, we can show that we can take the common stability margin (i.e., exponential decay rate) λ and the overshoot constant c to be

$$\lambda := \frac{1}{2}\underline{D}_1, \quad c = \sqrt{\frac{k+1 + \sqrt{(k-1)^2 + \overline{D}_1^2}}{k+1 - \sqrt{(k-1)^2 + \overline{D}_1^2}}}.$$

Finding an L satisfying the second hypothesis in Lemma 1 is straightforward: $\|A(t)\|$ is the largest singular value of $A(t)$, which depends on the choice of k .

Furthermore, exponential stability of the LTV system (50) means that its state transition matrix $\Phi(\cdot, \cdot)$ satisfies

$$\|\Phi(t, s)\| \leq \bar{c}e^{-\bar{\lambda}(t-s)} \quad (52)$$

for some $\bar{c}, \bar{\lambda} > 0$. The proof of Lemma 1 in [16] yields the following estimates for the overshoot \bar{c} and decay rate $\bar{\lambda}$: $\bar{c} := \sqrt{\beta_2/\beta_1}$ and $\bar{\lambda} := (1/\beta_2) - 2\beta_2^2\mu/\beta_1$, where $\bar{\lambda} > 0$ in light of (51).

The actual system (46) is the LTV system (50) driven by the perturbation (48). It is well known and easy to show that, as long as the exponential stability bound (52) is valid, $\bar{c}/\bar{\lambda}$ is the system's \mathcal{L}_∞ -induced gain, and for bounded perturbations satisfying $|\nu(t)| \leq \bar{\nu} \forall t$ for some $\bar{\nu} > 0$, the solutions of (46) satisfy

$$\left| \begin{pmatrix} \bar{\omega}_1(t) \\ \bar{\delta}_1(t) \end{pmatrix} \right| \leq \bar{c}e^{-\bar{\lambda}t} \left| \begin{pmatrix} \bar{\omega}_1(0) \\ \bar{\delta}_1(0) \end{pmatrix} \right| + \frac{\bar{c}}{\bar{\lambda}}\bar{\nu} \quad \forall t \geq 0. \quad (53)$$

Now, we can finish the analysis as follows. Given some range of initial conditions and the desired range in which we want the solution of our system (46) to belong, we can determine sufficiently small upper bounds M and ε on $\xi_1(t)$ and on $D'_1(\cdot)$, respectively, such that the magnitude of $\nu(t)$ in (48) (which depends on these two upper bounds as well as on the chosen range of ω_1 around ω_0 and the control gain k) is upper-bounded by a small enough $\bar{\nu}$ so that (53) guarantees that the solution indeed remains in the desired range. Recalling (49) and decreasing the upper bound on $D'_1(\cdot)$ further if necessary, we can always ensure that the last hypothesis of Lemma 1 holds with μ satisfying (51).

For the follower, we define the control u_2 (similarly to Section 3.1) as

$$u_2 = \left(D_2(\theta_2(t)) - D_1(\theta_1(t) + d(t)) \right) \omega_2(t) - k(\theta_1(t) + d(t)) + k\omega_0 t + \xi_1(t).$$

We can then write the closed-loop dynamics of the follower as

$$\begin{aligned} \dot{\theta}_2 &= \omega_2, \\ \dot{\omega}_2 &= -D_1(\theta_1 + d(t))\omega_2 + u_1 - kd(t) + \xi_1(t). \end{aligned}$$

5.2. Synchronization analysis

With $e := \omega_2 - \omega_1$ we have

$$\dot{e} = -D_1(\theta_1 + d)e - \left(D_1(\theta_1 + d) - D_1(\theta_1) \right) \omega_1 - kd.$$

With $V(e) := \frac{1}{2}e^2$ we have

$$\dot{V} \leq -\underline{D}_1|e|^2 + |e|\phi(|d|)$$

where

$$\phi(r) := \max_{(\theta_1, \omega_1) \in \Omega, |d| \leq r} \left| \left(D_1(\theta_1 + d) - D_1(\theta_1) \right) \omega_1 \right| + kr$$

and Ω is a bounded set in which $\theta_1 \pmod{2\pi}$ and ω_1 evolve. From this we obtain

$$|e| > \phi(|d|)/\underline{D}_1 \Rightarrow \dot{V} < 0$$

which gives ISS from d to e with ISS gain function $\phi(\cdot)/\underline{D}_1$. This implies, in particular, that

$$\limsup_{t \rightarrow \infty} |e(t)| \leq \frac{1}{\underline{D}_1} \phi \left(\limsup_{t \rightarrow \infty} |d(t)| \right).$$

The fact that the ISS gain depends on a compact set in which the state of the leader system evolves makes the synchronization error dynamics *quasi-ISS* with respect to d , in the sense of [25]. This situation is more subtle than the one we had in Section 3.2.

6. Concluding Remarks

In this paper, we proposed a method for synchronizing two electric power generators that is robust against disturbances in the measurements on which the method relies. Our approach is based on casting the synchronization problem as an observer design problem for two systems, a leader system and a follower system. The basic idea is that, by appropriately adjusting the control input of the follower system according to phase measurements of the leader system, its closed-loop dynamics act as a reduced-order observer that emulates the dynamics of the leader system. We showed that this approach can be used to achieve successful synchronization of electric power generators, and we also showed that robust synchronization is achieved when the phase measurements are corrupted by errors. Analytical and numerical results were used to validate the proposed robust synchronization method, and although we do not present this additional result here, robust synchronization was achieved when the proposed method was tested on a system modeled using a high-order generator model.

References

- [1] Ajala, O., Domínguez-García, A., Sauer, P., Liberzon, D., 2019a. Robust synchronization of electric power generators. URL: <https://arxiv.org/abs/1909.04095>.
- [2] Ajala, O., Domínguez-García, A., Sauer, P., Liberzon, D., 2019b. A second-order synchronous machine model for multi-swing stability analysis, in: Proc. of the North American Power Symposium, Wichita, KS.

- [3] Ajala, O., Domínguez-García, A.D., Liberzon, D., 2018. An approach to robust synchronization of electric power generators, in: Proc. of IEEE Conference on Decision and Control, Miami, FL, pp. 1586–1591.
- [4] Andrievskii, B., Fradkov, A.L., 2006. Method of passification in adaptive control, estimation, and synchronization. *Autom. Remote Control* 67, 1699–1731.
- [5] Andrievsky, B., Fradkov, A.L., Liberzon, D., 2017. Robustness of Pecora-Carroll synchronization under communication constraints. *Systems Control Lett.* 111, 27–33.
- [6] Arcak, M., 2007. Passivity as a design tool for group coordination. *IEEE Transactions on Automatic Control* 52, 1380–1390.
- [7] Carroll, T.L., 2005. Chaotic systems that are robust to added noise. *Chaos* 15. Article 013901.
- [8] Chopra, N., Spong, M.W., Lozano, R., 2008. Synchronization of bilateral teleoperators with time delay. *Automatica* 44, 2142–2148.
- [9] Dörfler, F., Bullo, F., 2014. Synchronization in complex networks of phase oscillators: a survey. *Automatica* 50, 1539–1564.
- [10] Dörfler, F., Simpson-Porco, J.W., Bullo, F., 2016. Breaking the hierarchy: distributed control & economic optimality in microgrids. *IEEE Transactions on Control of Network Systems* 3, 241–253. URL: <http://arxiv.org/abs/1401.1767>.
- [11] Fradkov, A.L., Andrievsky, B., Ananyevskiy, M.S., 2015. Passification based synchronization of nonlinear systems under communication constraints and bounded disturbances. *Automatica* 55, 287–293.
- [12] Fradkov, A.L., Andrievsky, B., Evans, R.J., 2008. Controlled synchronization under information constraints. *Physical Review E* 78, 036210.
- [13] Gao, X., Liberzon, D., Liu, J., Başar, T., 2018. Unified stability criteria for slowly time-varying and switched linear systems. *Automatica* 96, 110–120.
- [14] IEEE, 2006. IEEE guide for operation and maintenance of turbine generators. *IEEE Std 67-2005 (Revision of IEEE Std 67-1990)*, 1–69.
- [15] IEEE, 2009. IEEE application guide for IEEE Std 1547(tm), IEEE standard for interconnecting distributed resources with electric power systems. *IEEE Std 1547.2-2008*, 1–217.
- [16] Ioannou, P., Sun, J., 1996. *Robust Adaptive Control*. Prentice-Hall, New Jersey.
- [17] Jiang, X., Zhang, J., Harding, B.J., Makela, J.J., Domínguez-García, A.D., 2013. Spoofing GPS receiver clock offset of phasor measurement units. *IEEE Transactions on Power Systems* 28, 3253–3262.
- [18] Kundur, P., Balu, N.J., Lauby, M.G., 1994. *Power System Stability and Control*. McGraw-Hill.
- [19] Kuramoto, Y., 1975. Self-entrainment of a population of coupled nonlinear oscillators, in: Araki, H. (Ed.), *International Symposium on Mathematical Problems in Theoretical Physics*. Springer Berlin Heidelberg. volume 39 of *Lecture Notes in Physics*, pp. 420–422.
- [20] Nijmeijer, H., Mareels, I., 1997. An observer looks at synchronization. *IEEE Transactions on Circuits and Systems I* 44, 882–890.
- [21] Pecora, L.M., Carroll, T.L., 2015. Synchronization of chaotic systems. *Chaos: An Interdisciplinary Journal of Nonlinear Science* 25, 097611.
- [22] Pogromsky, A., Nijmeijer, H., 1998. Observer-based robust synchronization of dynamical systems. *Int. J. Bifurcation and Chaos in Applied Sciences and Engineering* 8, 2243–2254.
- [23] Polyak, B.T., Kvinto, Y.I., 2017. Stability and synchronization of oscillators: New Lyapunov functions. *Automation and Remote Control* 78, 1234–1242.
- [24] Schiffer, J., Ortega, R., Astolfi, A., Raisch, J., Sezi, T., 2014. Conditions for stability of droop-controlled inverter-based microgrids. *Automatica* 50, 2457–2469.
- [25] Shim, H., Liberzon, D., 2016. Nonlinear observers robust to measurement disturbances in an ISS sense. *IEEE Trans. Automat. Control* 61, 48–61.
- [26] Simpson-Porco, J.W., Dörfler, F., Bullo, F., 2013. Synchronization and power sharing for droop-controlled inverters in islanded microgrids. *Automatica* 49, 2603–2611.
- [27] Sontag, E.D., 1989. Smooth stabilization implies coprime factorization. *IEEE Transactions on Automatic Control* 34, 435–443.
- [28] Thompson, M.J., 2012. Fundamentals and advancements in generator synchronizing systems, in: Proc. of the Conference for Protective Relay Engineers, pp. 203–214.
- [29] Trip, S., Bürger, M., De Persis, C., 2016. An internal model approach to (optimal) frequency regulation in power grids with time-varying voltages. *Automatica* 64, 240–253.
- [30] Weitenberg, E., De Persis, C., 2018. Robustness to noise of distributed averaging integral controllers in power networks. *Systems & Control Letters* 119, 1–7.
- [31] Wood, A., Wollenberg, B., 1984. *Power Generation, Operation, and Control*. Wiley.
- [32] Zholbaryssov, M., Domínguez-García, A.D., 2016. Exploiting phase cohesiveness for frequency control of islanded inverter-based microgrids, in: Proc. of the IEEE Conference on Decision and Control, pp. 4214–4219.